

Extinction Characteristics of Cup-Burner Flame in Microgravity

Viswanath R. Katta*
 Innovative Scientific Solutions Inc.
 2766 Indian Ripple Road, Dayton, OH 45440

Fumiaki Takahashi
 National Center for Microgravity Research on Fluids and Combustion
 NASA Glenn Research Center
 21000 Brookpark Road, Cleveland, OH 44135

and

Gregory T. Linteris
 Fire Research Division, National Institute of Standards and Technology
 Gaithersburg, MD 20899

Abstract:[?]

Carbon dioxide extinguishes flames through dilution process. The extinction characteristics of CO₂ were previously studied using a cup-burner flame under normal-gravity conditions. As the diffusion flames behave differently in microgravity compared to those on earth, it is important to understand the structure of cup-burner flame and the extinction characteristics of CO₂ for 0g conditions. A numerical study was performed in the present paper using a time-dependent, axisymmetric mathematical model and by incorporating detailed chemical kinetics of CH₄ and O₂. Calculations were performed for the cup-burner flame under different gravitational forces. It was observed that the cup-burner flame ceases to flicker under gravitational forces less than 0.5g. As the buoyancy force was reduced, the flame diameter increased, the tip of the flame opened, and the flame at the base became vertical. Through numerical experiments it was found that radiative heat loss was solely responsible for the extinction of flame in the tip region under 0g conditions. In contrast, 1g flames were not affected much by the radiative heat losses. Calculations were made by adding CO₂ to air stream to obtain the limiting volume fraction of CO₂ for extinguishing the 0g flame. Similar to that observed in 1g flames, addition of CO₂ destabilized the flame base, which then moved downstream in search of a new stabilization location. For CO₂ volume fractions greater than 19.1 %, the flame base moved out of the computational area, as it could not find a stabilization point within the domain. This limiting concentration for 0g flame is ~ 32% higher than that obtained for the same flame under normal-gravity conditions. Calculations made by ignoring radiation for the limiting flame under 0g conditions yielded a stable flame. This study suggested that it is important to consider radiation while

estimating the extinction limits of cup-burner flames in microgravity.

Introduction:

A fire, whether within a spacecraft or in an occupied space on extraterrestrial bases can lead to mission termination or loss of life. The advent of longer duration missions to the moon, Mars, or aboard the space stations increases the likelihood of fire mishaps. Therefore, development of efficient fire safety systems and procedures represents a mission-critical task. Trifluorobromomethane (CF₃Br, Halon 1301) is a widely used¹ fire-suppressing agent and numerous studies have been conducted for understanding its inhibitory mechanism.²⁻⁴ However, it is also extremely effective for depleting stratospheric ozone. Consequently, with the current ban on the production of CF₃Br, replacements that are predominantly fluorinated hydrocarbons are being considered.⁵ Understanding the inhibition mechanisms of these replacements along with CF₃Br and inert agents is important for their efficient use and for developing new agents.

Studies conducted to gain an understanding of the inhibitory effects of halogenated hydrocarbons on flames have been performed in premixed^{6,7} and diffusion systems.^{8,9} Premixed flames are selected mainly because the overall reaction rate, heat release, and heat and mass transport can be described with a fundamental parameter—the laminar burning velocity; on the other hand, most common fires are of the diffusion type and often become dynamic in nature with large vortical structures entraining additional surrounding air.

The predominant experimental techniques for studying fire-suppression in diffusion flames are the cup-burner and opposing-jet configurations. In both these experiments, agents are quasi-statically added to either the fuel or air stream. The opposed-jet configuration offers very simple flames that can be modeled using one-dimensional analysis and, hence, is often used for the development of chemical kinetics models for different agents. From a fire safety point of view,

*Corresponding author: vrkatta@erinet.com

This paper is declared a work of the U.S. Government and is not subjected to copyright protection in the U.S.

however, the most hazardous situation is a low-strain-rate diffusion flame such as the one established over a cup burner where flames are more stable and larger concentrations of agent are required to achieve extinction. Studies on cup-burner flames are also important since the amount of agent required for extinguishing these flames is believed to scale to the requirements in common fires.

Under normal gravitational conditions, a laminar jet diffusion flame formed over a cup burner with a negligibly small fuel flow rate and a low-speed annular air flow develops large-scale, low-frequency (1-40 Hz), organized buoyancy-induced vortices on the air side of the flame. Both experimental^{10,11} and numerical¹² studies have been performed on these dynamic flames to identify the differences in agent requirements established using opposing-jet and cup-burner flames. On the other hand, several studies^{13,14} have pointed out that the low-speed, coaxial, jet diffusion flames similar to those associated with cup burners behave differently under microgravity. As a result, the agent requirements for extinguishing the cup-burner flames could be different from those established based on ground-based studies.

Several numerical investigations of dynamic jet flames were performed in the past using the conserved-scalar, global-chemistry, and detailed chemistry models, and have revealed important aspects of combustion such as the effect of heat-release rate,¹⁵ the role of buoyancy,^{14,16} enhancement of soot formation,¹⁷ and Lewis-number effects.^{18,19} Authors have recently performed comprehensive computations for the prediction of the effects of fire-suppressing agents [CO_2 , CF_3H and $\text{Fe}(\text{CO})_5$] on methane jet diffusion flames using detailed chemical-kinetics mechanisms.^{12,20,21}

This paper describes an investigation performed using a two-dimensional numerical model with detailed kinetics, developed for the simulation of dynamic jet diffusion flames, for establishing extinction criterion of cup-burner flames in microgravity. Carbon dioxide is used as a fire suppressing agent and is added to the air stream. Numerical experiments are performed to understand the dramatic structural differences observed between the cup-burner flames operating under normal- and micro-gravity conditions.

Description of Cup Burner:

The cup burner, described previously,^{10,11,12} was used for the present investigations on gravity effects on flame extinction. It consists of a cylindrical glass cup (28-mm diameter) positioned inside a glass chimney (53.3-cm tall, 9.5-cm diameter). To provide uniform flow, 6-mm glass beads fill the base of the chimney, and 3-mm glass beads (with two 15.8 mesh/cm screens on top) fill the fuel cup. Gas flows were measured by mass flow

controllers (Sierra 860¹), which were calibrated so that their uncertainty is 2 % of indicated flow. (All uncertainties are expressed as expanded uncertainties with a coverage factor of two.) To determine the extinction condition, the co-flowing air was held constant at (41.6 \pm 0.8) L/min, and CO_2 was added to the flow (in increments of < 1 % near extinction) until lift-off was observed. The air velocity in the absence of CO_2 is (10.7 \pm 0.21) cm/s, and the fuel jet velocity is (0.921 \pm 0.018) cm/s. The test was repeated at least three times. The fuel gas is methane (Matheson UHP, 99.9 %), the agent is CO_2 (Airgas), and the air is house compressed air (filtered and dried) which is additionally cleaned by passing it through an 0.01 μm filter, a carbon filter, and a desiccant bed to remove small aerosols, organic vapors, and water vapor.

Computational Model:

A time-dependent, axisymmetric mathematical model known as UNICORN (Unsteady Ignition and Combustion using ReactionNs)²² is used for the simulation of unsteady jet diffusion flames associated with the cup burner. It solves for axial and radial (z and r) momentum equations, continuity, and enthalpy- and species-conservation equations on a staggered-grid system. The body-force term due to the gravitational field is included in the axial-momentum equation to simulate upward-oriented flames. A clustered mesh system is employed to trace the gradients in flow variables near the flame surface. A detailed chemical-kinetics model GRI-V1.2 (developed by the Gas Research Institute)²³ is incorporated in UNICORN for the investigation of CO_2 effects on methane combustion. This mechanism for methane flames is comprehensive, with 31 species and 346 elementary reactions. Thermophysical properties such as enthalpy, viscosity, thermal conductivity, and binary molecular diffusion of all the species are calculated from the polynomial curve fits developed for the temperature range 300 - 5000 K. Mixture viscosity and thermal conductivity are then estimated using the Wilke and Kee expressions, respectively. Binary-type diffusion is assumed with the diffusion velocity of a species calculated using Fick's law and the effective-diffusion coefficient of that species in the mixture. A simple radiation model based on optically thin-media assumption was incorporated into the energy equation. Only radiation from CH_4 , CO , CO_2 , and H_2O was considered in the present study.²⁴

The finite-difference forms of the momentum equations are obtained using an implicit QUICKEST scheme,¹⁴ and those of the species and energy equations

¹ Certain commercial equipment, instruments, or materials are identified in this paper to adequately specify the procedure. Such identification does not imply recommendation or endorsement by NIST nor does it imply that the materials or equipment are necessarily the best available for the intended use.

are obtained using a hybrid scheme of upwind and central differencing. At every time-step, the pressure field is accurately calculated by solving all the pressure Poisson equations simultaneously and utilizing the LU (Lower and Upper diagonal) matrix-decomposition technique. The boundary conditions are treated in the same way as that reported in earlier paper.²⁵

Unsteady axisymmetric calculations for the cup-burner flames are made on a physical domain of 200 x 47.5 mm utilizing a 251 x 101 non-uniform grid system that yielded 0.2-mm grid spacing in both the z and r directions in the flame zone. The computational domain is bounded by the axis of symmetry and a wall boundary in the radial direction and by the inflow and outflow boundaries in the axial direction. The outer boundary in z direction is located sufficiently far from the burner exit (~ 7.5 fuel cup diameters) such that propagation of boundary-induced disturbances into the region of interest is minimal. Flat velocity profiles are imposed at the fuel and air inflow boundaries, while an extrapolation procedure with weighted zero- and first-order terms is used to estimate the flow variables at the outflow boundary. For the accurate simulation of flow structure at the base of the flame, which is very important in the flame-extinction studies, the fuel cup wall was treated as a 1-mm long and 1-mm thick tube in the calculations. The temperature of this tube was set at 600 K, which is very close to that measured in the experiment.

Simulations were performed on a Pentium III-1-GHz-based Personal Computer with 1 GB of memory. Typical execution time was ~ 52 s/time-step. Stably oscillating flames were obtained in about 3000 time-steps (which corresponds to 300 ms real time).

Results and Discussion:

Uniform flow of non-premixed reactants in a cup burner results in an axisymmetric, laminar diffusion flame. Typically, very low velocities are used for the reactant flows in these burners such that the flame generated is quite stable and its structure is similar to that of the uncontrolled fires. Under the influence of gravitational force, the low annular air velocity promotes the buoyancy-induced instabilities outside the flame surface and makes the flame to flicker at a low frequency. Several calculations were made to understand the structure and extinction characteristics of these dynamic flames for 1g conditions.

Flame Dynamics under Normal Gravity:

The fuel and air velocities of 0.921 and 10.7 cm/s, respectively, used in the present investigation represent a weakly strained flame. The computed instantaneous flowfield of the pure CH_4 /air flame is shown in color in Fig. 1. The CO_2 -iso-molar-concentration and temperature distributions are shown on the left and right halves, respectively. The velocity and iso contours of H_2

are superimposed on the temperature and CO_2 distributions, respectively. Except in the base region ($0.1 < z < 4$ mm), the peak temperature of the flame is constant everywhere at 1880 K. The flame height at the instant shown in Fig. 1 is ~ 64 mm.

The striking features of this flame are 1) low-frequency, large-amplitude oscillations in flame height and 2) significant inward curvature on flame surface at the base. Because of the gravity term in the axial-momentum equation and the low-speed annular-air flow (10.7 m/s), solution of the governing equations resulted in large toroidal vortices outside the flame surface. As these naturally formed vortices convect downstream, they force the flame to squeeze at certain locations and bulge at others and cause the flame height to increase and decrease. It is important to note that no artificial perturbation is used in the calculations for the development of these outer vortices. In the presence of gravitational force, acceleration of hot gases along the flame surface generated the vortical structures as part of the solution. Even though, these vortices (or instabilities) start to form upstream in the flame near the base region, they develop into recognizable vortical structures only in the farther downstream locations ($z > 50$ mm). However, due to the formation and convection of the vortices, the flame surface oscillates radially at every location with varying intensity. The frequency corresponding to the passage of these vortices (also known as the flame-flickering frequency) is ~ 11 Hz. The low fuel velocity and the large fuel-cup diameter are responsible for making the flame to curve inwardly at the base. As a result the velocity at the flame base no longer remained parallel to the flame surface.

Evolutions of the flame at two different heights above the burner are shown in Fig. 2 by plotting the radial distribution of temperature at different times. While the image in Fig. 1 represents the flame structure for a part of the flame domain at $t = 0$ ms, that in Fig. 2 represents the temperature at two locations for approximately one cycle ($0 \text{ ms} < t < 100 \text{ ms}$). At $z = 30$ mm, the flame is oscillating radially, along with a weak fluctuation of fuel jet at the center. However, the vortices formed outside the flame surface have grown significantly by the time they reached a height of 80 mm and are pinching off a portion of fuel from the fuel jet. The detached fuel mass is burning separately as it convects downstream. A comparison between evolutions at 30 and 80 mm reveals that the period of oscillation at the former location is ~ 105 ms ($f \sim 9.5$ Hz) while that at the latter location is ~ 93 ms ($f \sim 10.8$ Hz).

Extinction Characteristics under Normal Gravity:

To evaluate the extinction performance of CO_2 in this flame, a number of calculations were performed for increasing amounts of CO_2 in the air stream, with a constant co-flowing gas velocity at the cup rim. Addition of CO_2 was compensated by a reduction in the amount of air for keeping the total flow rate (or velocity)

constant. These calculations suggested that when the CO₂ volume fraction was < 10 % (i.e., oxygen > 18.9 % and nitrogen > 71.1 %), no significant change to the flame shape was observed.¹² For concentrations between 10 and 14.5 %, the flame was separated (< 4 mm) from the burner lip and stabilized at a new location. An instantaneous solution of the computed flame for 14.5 % CO₂ is shown in Fig. 3. The variables shown here are same as those shown in Fig. 1. As evident from this plot, the flame base has been moved inside and downstream of the burner lip by ~ 4 mm. Interestingly, the flame oscillation in the base region has increased significantly. As a result, the base of the flame moved back and forth between the burner lip and the location shown in Fig. 3 with time. The separation between the burner lip and the flame base allowed more air and CO₂ to enter the flame and provided partially premixed flow conditions. When the concentration of the added CO₂ was increased to a value > 14.5 %, the flame was completely blown out of the computational domain. The experimental result for the extinction volume fraction of CO₂ in the air stream is 0.161 ± 0.005 for an oxidizer stream velocity of 10.7 cm/s. Hence, the calculated extinction volume fraction of 14.5 % agrees reasonably well with that measured in the experiment.

Calculations made with different CO₂ concentrations indicate that the cup-burner flame extinguishes through the blowout process—meaning that, the flame at the base detaches from the burner first, similar to lifting of jet diffusion flames,²⁶ and then shifts downstream till it clears off from the computational domain. This blowout behavior was the same for all the cases with CO₂ concentration > 14.5 %. The extinction limit obtained for cup-burner flame is compared with those obtained for opposing-jet flames in Fig. 4. The variations of flame temperature and peak CO₂ produced in the flame zone as functions of added CO₂ are shown for two differently strained opposing-jet flames. The temperature of the low-strain flame with 0 % CO₂ added is slightly above that of the cup-burner flame while that of the moderate-strain flame is slightly below. Consistent with these temperatures, the limiting volume fraction of CO₂ for the cup burner (14.5 % computed) falls between the two cases, but nearer to the low-strain opposed-jet flame extinction volume fraction (16.4 %).

Flame Structure under Microgravity:

The gravitational force acting on the cup-burner flames in Figs. 1 and 3 caused the flow to accelerate and induced flow instabilities. Earlier studies on jet diffusion flames in microgravity^{13,14} suggest that flames tend to become steady in nature and short in height as the gravitational force acting on them decreases. To investigate the effects of gravitational force on cup-burner flames, calculations were repeated for different gravitational-force conditions. Results for 0.5g, 0.1g and 0g are shown in Figs. 5(a), 5(b), and 5(c), respectively. Concentrations of CO₂ and H₂ are shown on the left

halves in these figures while the velocity field and temperature are shown on the right halves. Note, the contour legends, color tables, and velocity-vector magnitudes used in these figures are identical to those used for 1g flame (Fig. 1).

The salient features noted from a comparison of flame structures obtained under different gravitational-force conditions are: 1) flames became steady state when gravitational force was < 0.5g, 2) flame height decreased and diameter increased with reduction in gravitational force, 3) peak velocity at a height of 80 mm above the burner decreased from ~2.2 m/s to ~0.2 m/s when gravity was reduced from 1g to 0g, 4) peak temperature decreased slightly but, more importantly, temperature of the flame tip decreased dramatically with reduction in gravitational force, and finally, 5) the severely concaved flame near the burner rim became parallel to the fuel jet when gravitational force was reduced from 1g to 0g.

Several investigators in the past have studied the relationship between the flame flicker and gravitational force.^{22,27} In general, the flickering flames were found to oscillate even at very low-gravity conditions. It was suggested that flicker frequency decreases with gravitational force raised to a power—typically, 0.5. Contrary to these findings, cup-burner flames seem to cease flicker when the gravitational force is reduced to 0.5g. Several attempts using smaller time steps and finer grids failed to yield a flickering flame for 0.5g. This suggests that buoyancy induced instability possesses a cut-off value on gravitational-force scale, below which they vanish. This is a characteristics of an absolute instability mode of a jet flow.²⁸ In a typical jet diffusion flame with a small-diameter, high-velocity fuel jet the cut-off gravitational force for losing absolute-instability mode is close to zero and was not captured in the calculations and experiments. However, the very low fuel jet velocity and a large-diameter fuel cup used in the present investigations seem to increase the limiting value to > 0.5g. Existence of such limiting value for the flame oscillations further confirms that buoyancy-induced instabilities are of absolute-instability type.

Flame structure shown in Fig. 5(c) for 0g case represents a open-tipped flame. In fact, decreasing gravitational force on a cup burner flame generated dramatic changes to its structure. At 1g, the flame was severely oscillating with pockets of fuel being pinched off from the jet and burning independently (Figs. 1 and 2). At 0.5g, a closed-tip, steady-state flame was generated [Fig. 5(a)]. Finally, for gravitational force < 0.2g, flame became completely open-tipped with burning taking place only in the shoulder region [Figs. 5(b) and 5(c)]. Formation of closed contours of 0.02 X_{H2} in these flames in the base region suggests that H₂ is no longer produced at the flame tip. The reasons for such flame opening at lower-g cases will be discussed in the next section.

Importance of Radiation under Microgravity:

As described earlier, radiation from CH_4 , CO , CO_2 , and H_2O was included in the present calculations. A simple radiation model based on optically thin-media assumption was used. As suggested by Easton et al.,²⁹ radiative heat losses could become a dominating heat-transfer mechanism when the generation of heat is decreased due to lack of reactant convection. To verify this, radial distributions of heat release rate and radiative heat loss at 20 mm above the burner are plotted in Fig. 6 for different g cases. This height represents the farthest location from the burner rim where flame exists in all g cases. Fig. 6 shows that heat release rate decreases significantly with reduction in gravitational force. For 0g case the maximum heat release rate is only $1/3^{\text{rd}}$ of that obtained for 1g case. Since, flame temperatures are nearly the same at this location for all the cases, reduction in heat release rate can be attributed to the reduction in reactant fluxes into the flame zone. The drastic decrease in convective flow in lower g cases is limiting the reactant fluxes in to the flame zone. On the other hand, radiative heat losses are more or less the same in all g cases. The dominance of radiative heat loss in low-g cases is causing the flame to extinguish in the downstream locations.

To further verify that the radiative heat losses are indeed causing the flame to extinguish at the tip, numerical experiments have been performed on 0g flame. Three different calculations were made for this flame: 1) by ignoring radiation in the energy equation, 2) by ignoring finite-rate chemistry, and 3) by ignoring both radiative heat loss and finite-rate chemistry. The flow conditions and numerical details used for these calculations were the same as those used for the flame (0g case) shown Fig. 5(c). All three calculations converged to steady-state flames even though unsteady simulations were performed.

The 0g flame computed with no radiation is shown in Fig. 7 with a plotting scheme same as that used for Fig. 5(c). Surprisingly, in the absence of radiation, flame became a closed-tip one with burning taking place along the flame surface from base to the tip at the centerline. The peak flame temperature has increased by ~ 150 K but, more interestingly, temperature all along the flame surface became nearly the same. The closed contours of H_2 in Fig. 5(c) disappeared in Fig. 7 indicating that combustion is taking place all the way up to the flame tip when the radiation is turned off in the calculations. Due to this increased burning (and volumetric expansion) the local velocity has increased by $\sim 35\%$ at $z = 80$ mm compared to that in 0g flame shown in Fig. 5(c).

Flames resulting from the calculations made by using infinitely-fast-chemical-kinetics model ($\text{CH}_4 + 2\text{O}_2 + 7.5\text{N}_2 \Rightarrow \text{CO}_2 + 2\text{H}_2\text{O} + 7.5\text{N}_2$) are shown in Fig. 8. The iso-temperature color plots of the flames without and with radiation are shown in the left and right halves, respectively. The structures of these flames became

similar to their counter parts computed with finite-rate chemistry. The infinitely fast chemistry flame computed with radiation is similar to the one shown in Fig. 5(c) and the flame computed without the radiative heat loss is similar to that shown in Fig. 7 (right side). These comparisons further suggest that finite-rate chemistry is not responsible for the tip quenching seen in 0g and low-g flames. Calculations were also performed for 0g flame by using unity-Lewis number assumption. The resulted flame with radiative heat losses had a flame structure that is similar to that shown in Fig. 5(c). This suggests that neither curvature nor preferential diffusion are responsible for the tip opening of the 0g flame. Analysis of all the results obtained from different numerical experiments suggests that radiative heat losses are solely responsible for the quenching phenomenon seen in microgravity cup-burner flames.

To understand how radiation is affecting only the low-g flames, calculations for the 1g flame were also repeated by turning off the radiative heat losses in the energy equation. The flame resulted from this simulation is shown in Fig. 9 using the plotting scheme that was adopted for Fig. 1. Even though, there exists some minor differences in the flame temperatures, over all, 1g flames obtained with (Fig. 1) and without (Fig. 9) the radiative heat losses are similar in structure. Tips of both the flames are closed with burning taking place all along the flame surface. Both the flames are flickering and resulting in pinching off of fuel pockets at the tip. However, the flickering frequency is increased to 12.5 Hz. when the radiative heat loss was ignored in the calculations. An additional vortex is forming in Fig. 9 in addition to those formed in Fig. 1. This should be expected as the buoyancy forces are slightly increased with an increase in flame temperature in Fig. 9.

The temperature and axial velocity along the flame surface obtained with and without radiation are plotted for the 0g flame in Fig. 10(a) and for the 1g flame in Fig. 10(b). In all the calculations temperature and axial velocity have increased initially in the flame base region. However, in case of 0g, flame temperature remained more or less constant around 2000 K in the downstream locations when radiation was ignored and decreased linearly from 1850 K when radiation was included in the calculations. It was found from earlier calculations¹² that stoichiometric methane diffusion flames quench when temperature is dropped below 1580 K. Based on this it can be assumed that the 0g flame (computed with radiative heat loss) was quenched at locations $z > 35$ mm. Absence of combustion in these locations resulted in a constant axial velocity of ~ 0.22 m/s, where as, it is increasing monotonically when radiation was turned off.

In the case of 1g flame, calculations made with and without the radiative heat losses yielded flame temperatures that are nearly constant [Fig. 10(b)]. In both calculations axial velocities are increasing with z due to buoyancy and thermal expansion of gases. The higher axial velocities in the case of 1g flame (~ 1 m/s

compared to 0.22 m/s in 0g case) are resulting in higher reactant fluxes into the flame zone and, in turn, increasing the heat release rates high enough to overcome the heat losses due to radiation. As a result, radiation did not have much effect on the 1g flame.

Extinction Characteristics under 0g:

Calculations made for 1g and 0g showed dramatic differences in the flame structures; mainly due to buoyancy and radiation. Because of this extinguishment of 0g flame through injection of CO₂ in air stream could be different from that of 1g flame shown in Figs. 3 and 4. To evaluate the performance of CO₂ in extinguishing 0g flames several calculations were made by adding CO₂ in different volume fractions to the air stream of the 0g flame shown in Fig. 5(c). The limiting volume fraction of CO₂ to extinguish the flame was found to be 19.1%. This limiting value is nearly 32% more than that was required for extinguishing the same flame under normal-gravity conditions. Results obtained with 5%, 10%, 15% and 19.1% of CO₂ are shown in Fig. 11. The plotting scheme used here is also same as that used for Fig. 3. Addition of CO₂ did not change the overall structure of the 0g flame. That is, for different volume fractions of CO₂ tip of the flame is opened and the entire flame remained vertical. However, as CO₂ volume fraction was increased the length of the vertical flame decreased.

Similar to 1g-flame quenching process, the primary role of CO₂ on 0g-flame quenching was to destabilize the flame base. As CO₂ was added to air stream, the flame got weaker and its temperature decreased. For smaller volume fractions (< 10%) of CO₂ flame base moved upstream closer to the burner rim and for moderate volume fractions ($0.1 < X_{CO_2} < 0.15$) it moved slightly downstream away from the burner rim. When CO₂ volume fraction was increased beyond 15%, flame base moved significantly and still found a new stabilization location in the flowfield. For volume fractions > 19.1% flame base became unstable and kept moving downstream in search of a new stabilizing location. As the flame could not find another stabilizing location it was completely cleared off from the computational domain--resulting in flame extinction. Like in 1g case, flame at 0g also did not extinguish before its base became unstable.

The location of flame base (obtained from peak temperature location in the base region) and the value of peak temperature are plotted in Fig. 12 for different concentrations of CO₂ and for both 1g and 0g cases. The limiting volume fractions of CO₂ for extinguishing these flames are also shown. It is clear from this plot that the extinguishment mechanisms of 0g and 1g flames are similar. In both the flames, the flame base moved closer to the burner rim initially and then moved away from the rim as CO₂ added to the air stream. On the other hand, flame-base temperature decreased monotonically with CO₂ concentration. There are some differences exist between the quenching processes taking place under 0g

and 1g conditions. First, the flame-base location under 1g conditions is more sensitive to the volume fraction of the added CO₂. This is probably due to the higher velocities at the flame base that were induced from strong entrainment in these buoyant flames. Secondly, the temperature of the flame base prior to extinguishment decreased rapidly in the case of 1g flame, while it decreased linearly in the case of 0g flame. Rapid decrease in flame temperature near extinction was also observed in the cases of opposing jet diffusion flames (Fig. 4). It is interesting to note that the base of 1g flame and opposing jet flame are subjected to stretching, where as, the base of a 0g flame is nearly unstretched. That means, the rapid (some times exponential) decrease in flame temperature near extinction observed in ground based experiments and in opposing jet flames is due to the inherent stretch present on these flames and only in microgravity one could find true limits (unaffected by stretch) for quenching.

To determine the effect of radiation on the near-extinction flame structure [Fig. 11(d)], calculations for the 0g flame with 19.1% CO₂ added in the air stream were repeated by turning off the radiative heat losses in the energy equation. The resulting flame is shown in Fig. 13 using the plotting scheme adopted from Fig. 11(d). Surprisingly, the tip of the flame became closed with burning taking place all along the flame surface between the burner rim and centerline when there is no radiative heat loss. The flame base also moved closer to the burner rim [cf. Figs. 13 and 11(d)] representing a more stable flame. That means, the extinction limit obtained by ignoring radiation would be greater than 19.1%. It also reminds the importance of considering radiation while determining the extinction limits.

Conclusions:

A periodically oscillating, pure-methane-air diffusion flame formed over a cup burner was used to explore the suppression characteristics of CO₂ under normal- and micro-gravity conditions. A detailed chemical-kinetics model GRI-V1.2 having 31 species and 346 elementary-reaction steps was incorporated into a time-dependent, axisymmetric CFD model for the investigation of the effects of CO₂ on methane combustion. Under normal-gravity conditions, the laminar cup-burner flame for a small fuel flow rate and a low-speed annular air flow, generated large-scale, low-frequency (~ 10 Hz), organized vortices on the air side of the flame. Calculations were performed for this flame under different gravitational forces. It was observed that the cup-burner flame ceases to flicker for gravitational forces less than 0.5g. As the buoyancy forces were reduced, the flame diameter increased, the tip of the flame extinguished (opened), and the flame at the base became vertical. Through numerical experiments it was found that radiative heat loss was solely responsible for the extinction of flame tip under 0g conditions. On the

other hand, ignoring radiation in 1g-flame calculation resulted a 25% increase in flicker frequency.

Calculations for the cup-burner flame were made by adding CO₂ to air stream to obtain the limiting volume fraction for extinguishing the 0g flame. Similar to that observed in 1g flames, addition of CO₂ destabilized the flame base, which then moved downstream in search of a new stabilization location. For CO₂ volume fractions greater than 19.1 %, the flame base moved out of the computational area, as it could not find a stabilization point within this domain. This limiting concentration for 0g flame is ~ 32% higher than that obtained for the same flame under normal-gravity conditions. Calculations made by ignoring radiation for the limiting flame under 0g conditions yielded a stable flame. It is important to consider radiation while estimating the extinction limits of cup-burner flames in microgravity.

Acknowledgements:

This work was supported by the Office of Biological and Physical Research, NASA, Washington, D. C. The first author would like to thank Dr. Mel Roquemore of Wright Laboratory for the stimulating discussions on buoyant flames.

References:

- Anderson, S. O., *Fire J.*, Vol. 81, 1987, p. 56 and 118.
- Gann, R. G. (Ed), *Halogenated Fire Suppressants*, ACS Symposium Series No. 16, The American Chemical Society, 1975.
- Biordi, J. C., Lazzara, C. P., and Papp, J. F., Fourteenth Symposium (International) on Combustion, The Combustion Institute, Pittsburgh, 1973, p. 367.
- Westbrook, C. K., *Combust. Sci. Technol.* Vol. 34, 1983, p. 201.
- Nyden, M. R., Linteris, G. T., Burgess, D. R. F., Jr., Westmoreland, P. R., Tsang, W., and Zachariah, M., in *Evaluation of Alternative In-Flight and Dry Bays* (Eds. W. L. Grosshandler, R. G. Gann, and W. M. Pitts), National Institute of Standards and Technology, Gaithersburg, MD, 1994, NIST SP 861, p. 467.
- Linteris, G. T., and Truett, L., *Combust. Flame*, Vol. 105, 1996, p. 15.
- Linteris, G. T., Burgess, D. R., Jr., Babushok, V., Zachariah, M., Tsang, W., and Westmoreland, P., *Combust. Flame*, Vol. 113, 1998, p. 164.
- Milne, T. A., Green, C. L., and Benson, D. K., *Combust. Flame*, Vol. 15, 1970, p. 255.
- Seshadri, K., and Ilincic, N., *Combust. Flame*, Vol. 101, 1995, p. 271.
- Hirst, B. and Booth, K., *Fire Technol.* 13:296 (1977).
- Linteris, G.T. and Gmurczyk, G.W., in *Fire Suppression System Performance of Alternative Agents in Aircraft Engine and Dry Bay Laboratory Simulations* (R.G. Gann, Ed.), National Institute of Standards and Technology, Gaithersburg, MD, 1995.
- Katta, V. R., Takahasi, F., and Linteris, G. T., *Proceedings of the 7th International Symposium on Fire Safety Science*, Worcester, MA, 16-21 June 2002.
- Hegde, U., Zhou, L., and Bahadori, Y. M., *Combustion Science and Technology*, Vol. 102, 1994, pp. 95-113.
- Katta, V. R., Goss, L. P., and Roquemore, W. M., *AIAA Journal*, Vol. 32, No. 1, 1994, p. 84.
- Ellzey, J. L., Laskey, K. J., and Oran, E. S., (1989), in *Dynamics of Deflagrations and Reactive Systems: Flames*, A. L. Kahl, J. C. Leyer, A. A. Borisov, and W. A. Sirignano, Eds., Vol. 131, *Progress in Astronautics and Aeronautics*, American Institute of Aeronautics and Astronautics, Washington, D. C., 1989, p. 179.
- Davis, R. W., Moore, E. F., Roquemore, W. M., Chen, L.-D., Vilimpoc, V., and Goss, L. P., *Combustion and Flame*, Vol. 83, Nos. 3/4, 1991, pp. 263-270.
- Kaplan, C. R., Oran, E. S., Kailasanath, K., and Ross, H. D., *26th Symposium (International) on Combustion*, The Combustion Institute, Pittsburgh, PA, 1996, p. 1301.
- Takagi T., and Xu, Z., *Combustion and Flame*, Vol. 96, Nos. 1 and 2, 1994, p. 50.
- Katta, V. R. and Roquemore, W. M., *Combustion and Flame*, Vol. 100, No. 1, 1995, p. 61.
- Katta, V. R., Takahasi, F., and Linteris, G. T., *Fire-Suppression Characteristics of CF3H in a Cup-Burner*, to be submitted to *Combustion and Flame*.
- Linteris, G. T., Katta, V. R., and Takahasi, F., *Experimental and Numerical Evaluation of Metallic Compounds for Suppressing Cup-Burner Flames*, to be submitted, 2003.
- Roquemore W. M., and Katta, V. R., *Journal of Visualization*, Vol. 2, Nos. 3/4, 2000, pp.257-272.
- Frenklach, M., Wang, H., Goldenberg, M., Smith, G. P., Golden, D. M., Bowman, C. T., Hanson, R. K., Gardiner, W. C., V. Lissianski, V., Technical Report No. GRI-95/0058, Gas Research Institute, Chicago, IL, November 1, 1995.
- Annon., *Computational Submodels*, International Workshop on Measurement and Computation of Turbulent Nonpremixed Flames., <http://www.ca.sandia.gov/tdf/Workshop/Submodels.html>, 2001.
- Katta, V. R., Goss, L. P., and Roquemore, W. M., *Int. J. Num. Methods Heat Fluid Flow*, Vol. 4, No. 5, 1994, p. 413.
- Takahashi, F., and Katta, V. R., *Proceedings of the Combustion Institute*, Pittsburgh, PA, Vol. 28, 2000, pp. 2071-2078.
- Bahadori, M. Y., Zhou, L., Stocker, D. P., and Hegde, U., *Proceedings of the 1996 Fall Technical Meeting of the Eastern States Section of the Combustion Institute*, 1996, pp. 451-454
- Raghu, S., and Monkewitz, P., *Physics of Fluids A*, Vol. 3, No. 4, 1991, pp. 501-503.
- Easton, J., Tien, J., and Dietrich, D., *First Joint Meeting of the U. S. Sections of the Combustion Institute*, Washington, D.C., March 14-17, 1999, pp. 665-668.

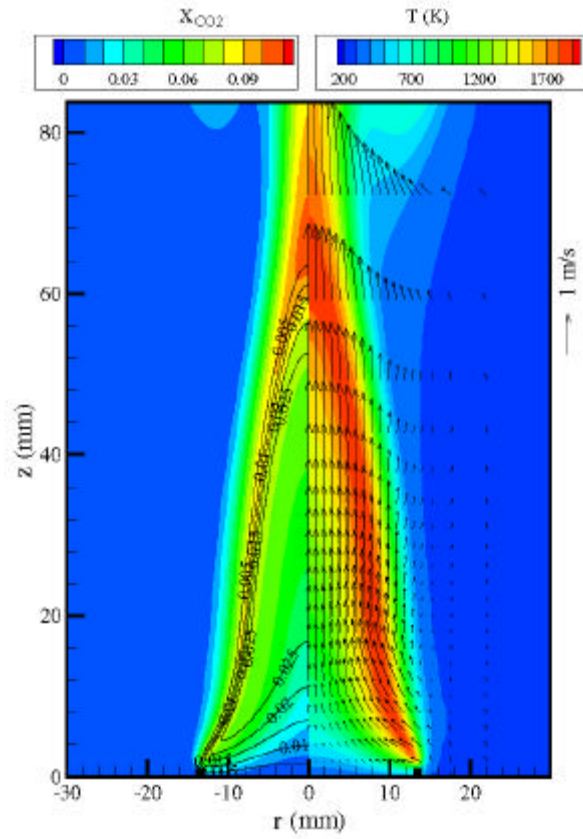


Fig. 1. Cup-burner flame simulated for normal-gravity conditions. Distributions of CO₂ concentration and temperature are plotted in left and right halves, respectively. Contours of H₂ concentration and velocity field are superimposed on left and right halves, respectively.

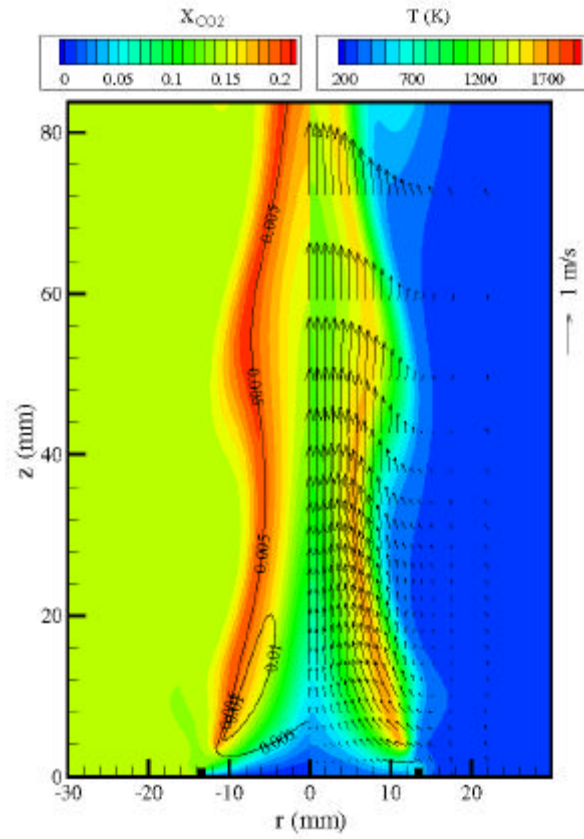


Fig. 3. Structure of the normal-gravity flame with near-extinction concentration of CO₂ added to the air stream. Temperature and velocity field are shown on right half and CO₂ and H₂ concentrations are shown on left half.

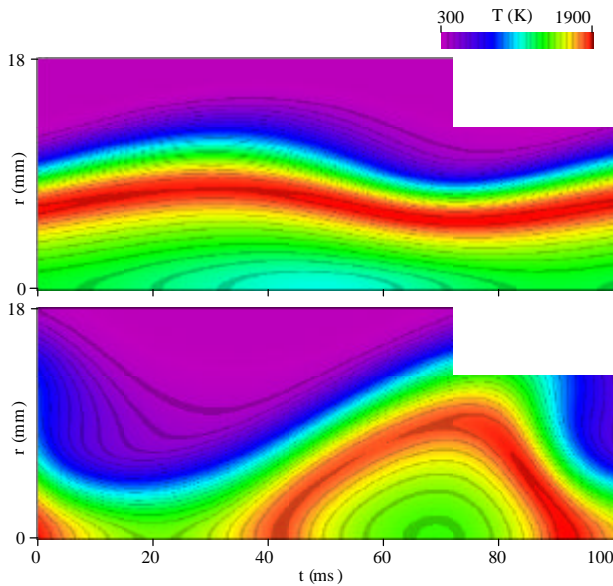


Fig. 2. Temperature evolution obtained at (a) 30 mm and (b) 80 mm above the burner exit. Flame flicker frequency is ~ 11 Hz.

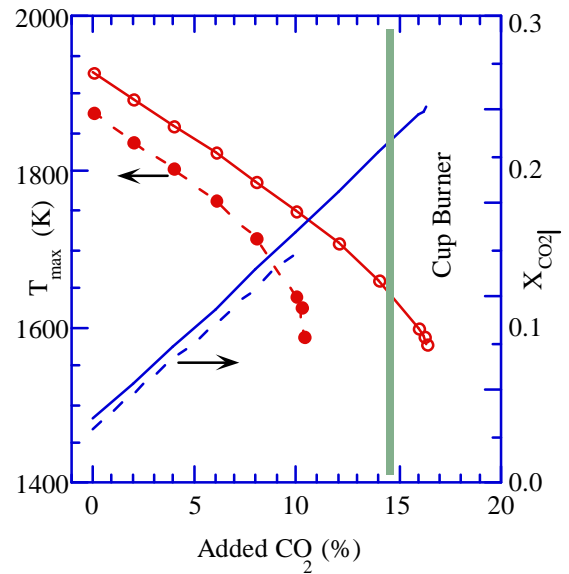


Fig. 4. Variations in flame temperature (T_{max}) and peak CO₂ concentration with the percentage of CO₂ added to air in counterflow diffusion flames. Limiting concentration for cup-burner is also marked.

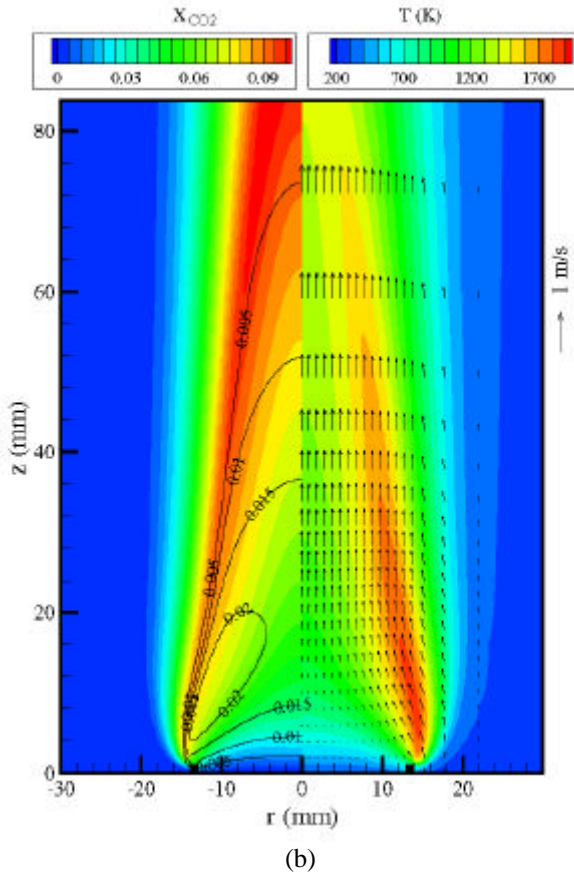
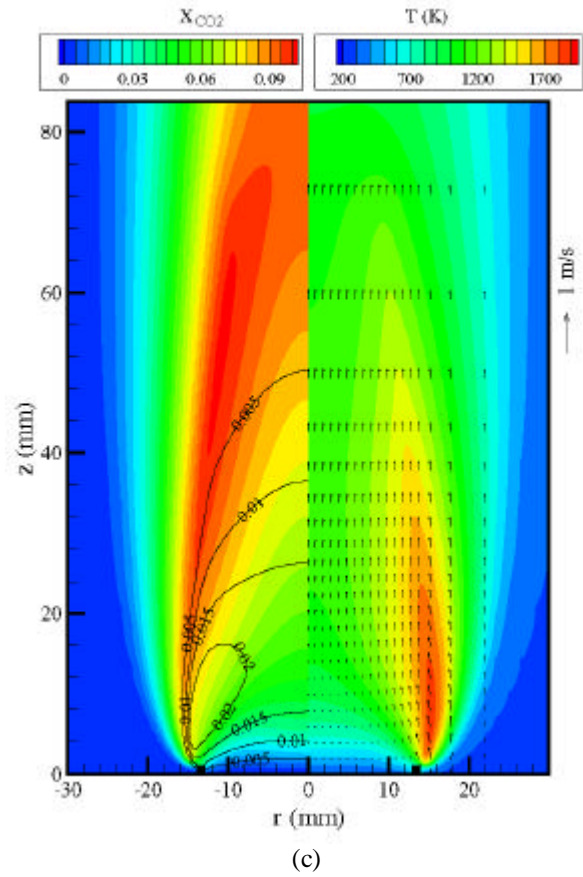
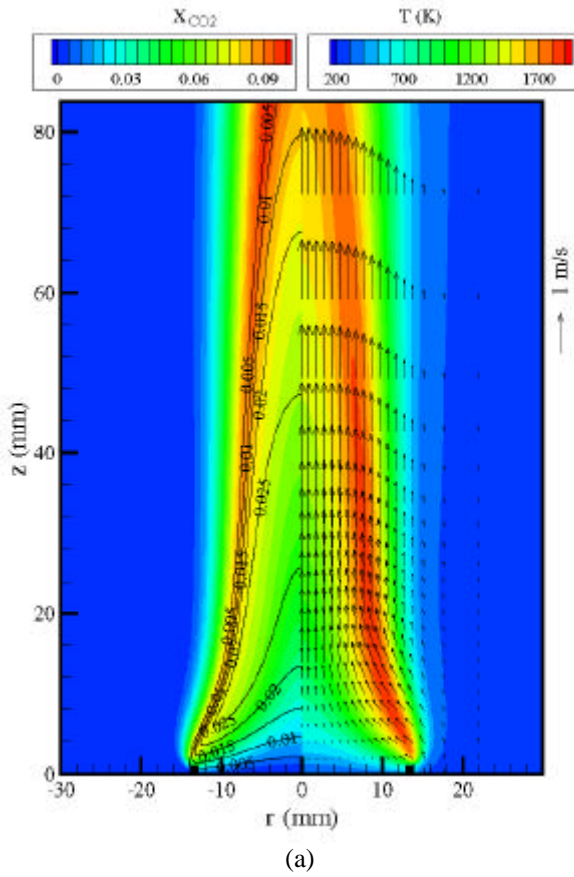


Fig. 5. Structures of cup-burner flame under (a) 0.5g, (b) 0.1g and (c) 0g conditions. Temperature and velocity fields are shown on right half and CO₂ and H₂ concentrations are shown on left half.

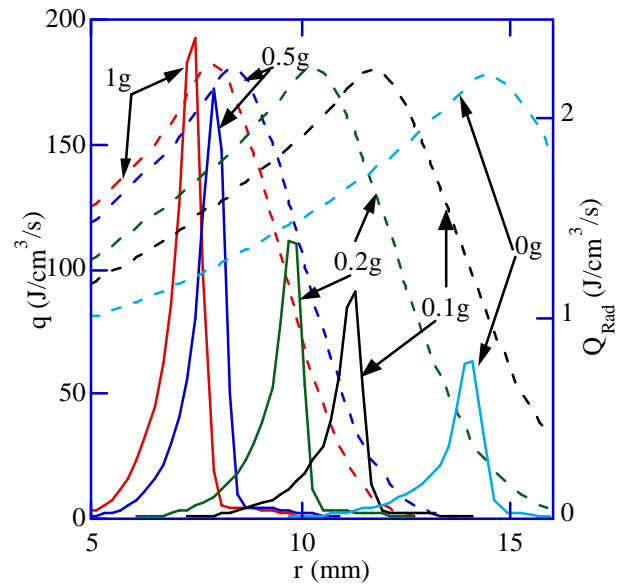


Fig. 6. Distributions of heat release rate q (solid lines) and radiative heat loss Q_{rad} (broken lines) at 20 mm above the burner under different gravitational conditions.

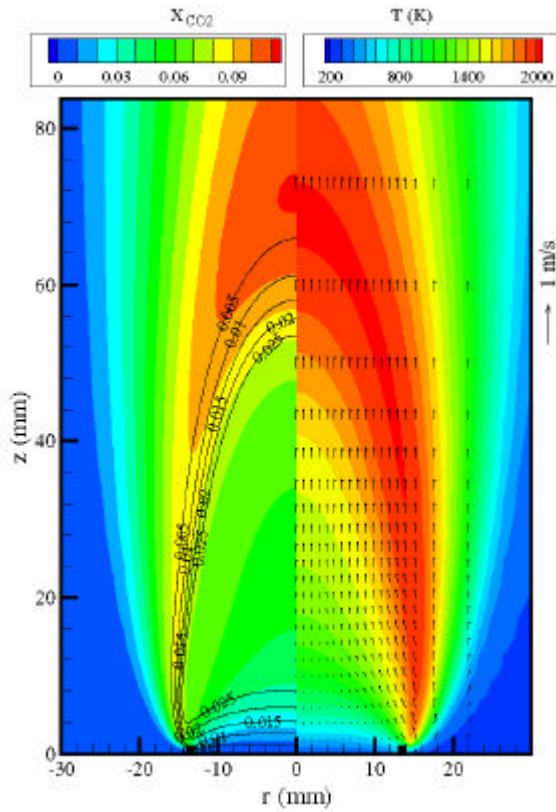


Fig. 7. Cup-burner flame under 0g conditions calculated by ignoring radiative heat losses.

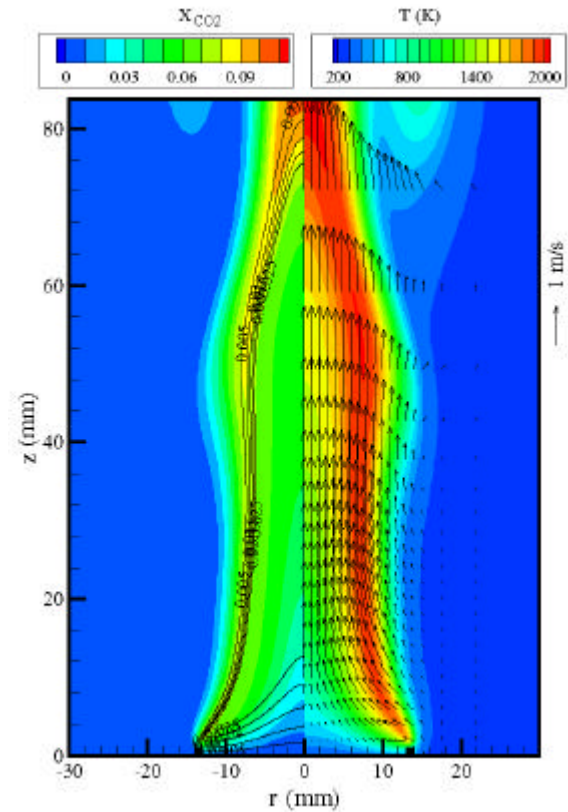


Fig. 9. Cup-burner flame under normal-gravity conditions calculated after ignoring radiative heat losses.

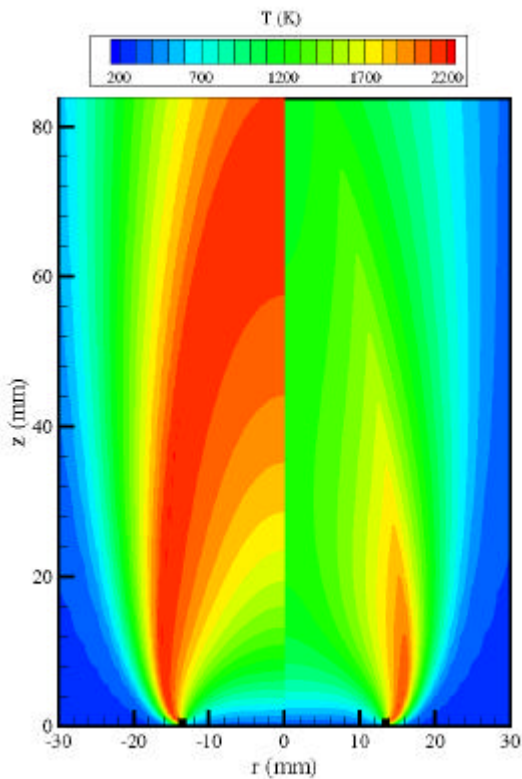


Fig. 8. Cup-burner flame under 0g conditions calculated with infinitely fast chemical kinetics. Flames without and with radiative heat losses are shown in left and right halves, respectively.

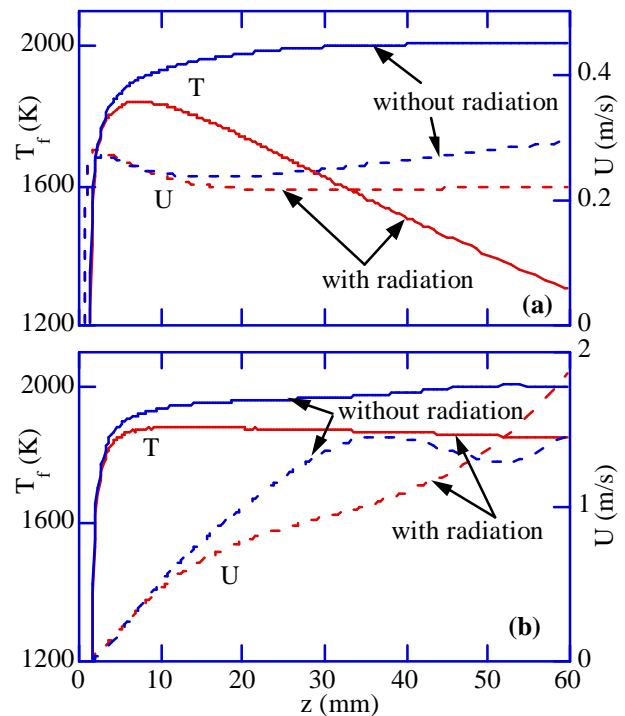


Fig. 10. Variations of temperature and axial velocity with height along the flame surface for (a) 0g and (b) 1g flames.

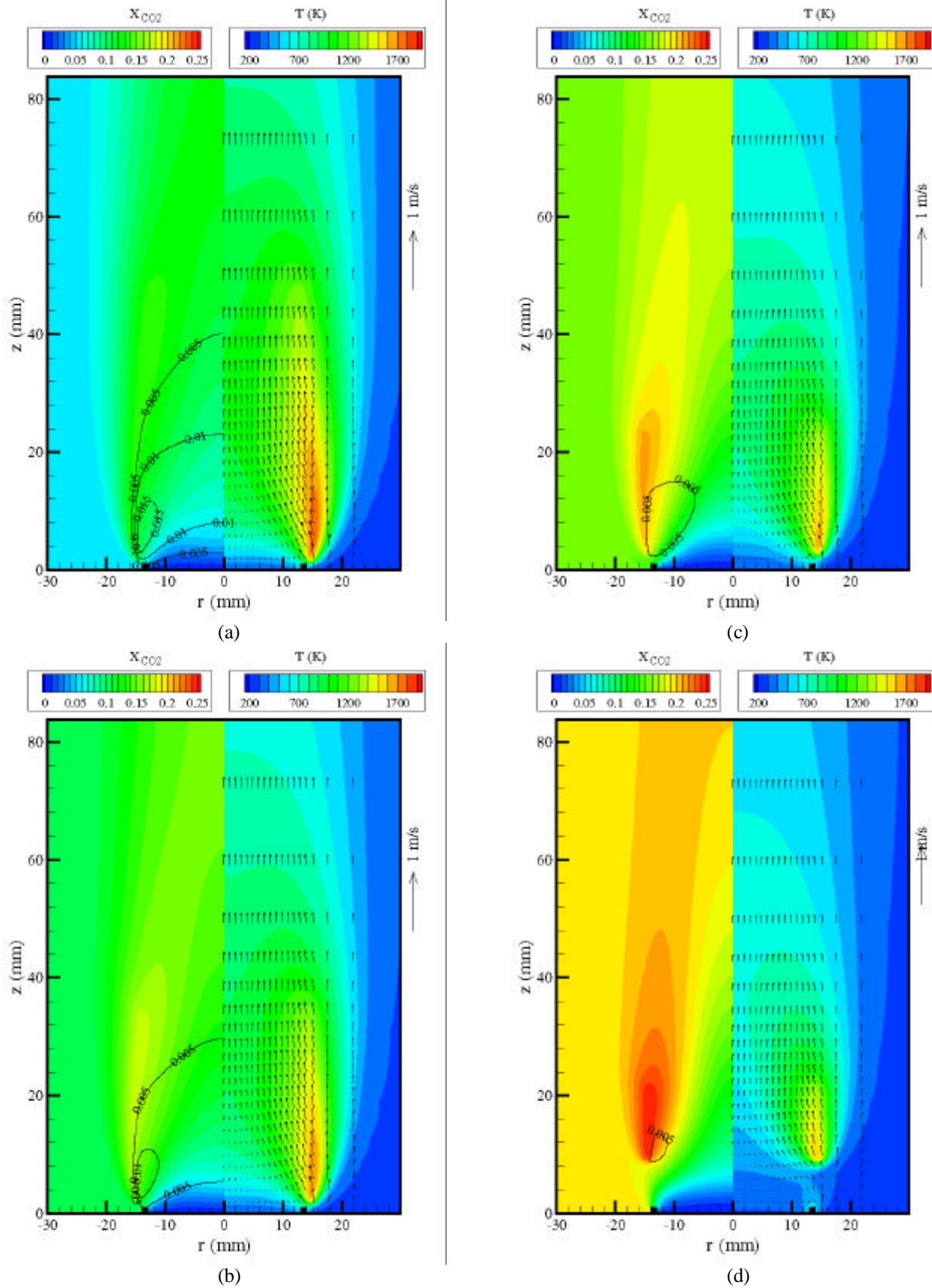


Fig. 11. Effect of CO_2 addition to airflow on the 0g cup-burner flame. (a) 5%, (b), 10%, (c) 15%, (d) limiting value of 19.1%. Temperature and velocity fields are shown on right half and CO_2 and H_2 concentrations are shown on left half.

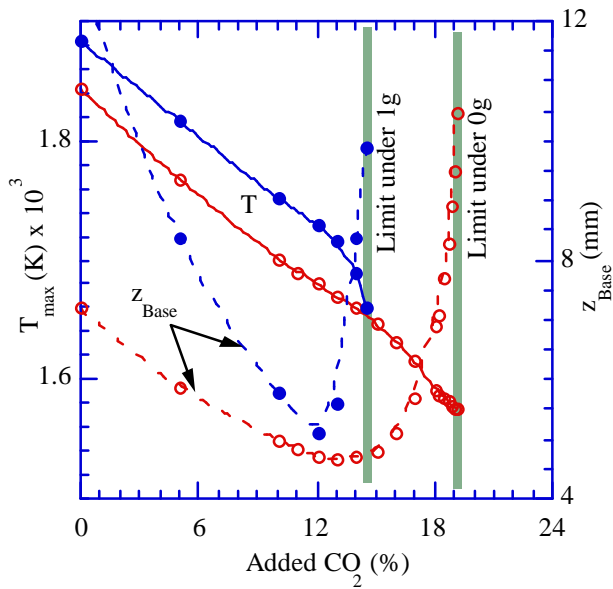


Fig. 12. Flame-base temperature and its distance from burner rim for different volume fractions of CO_2 in the air stream. Open symbols represent 0g conditions and solid symbols represent normal-gravity flames.

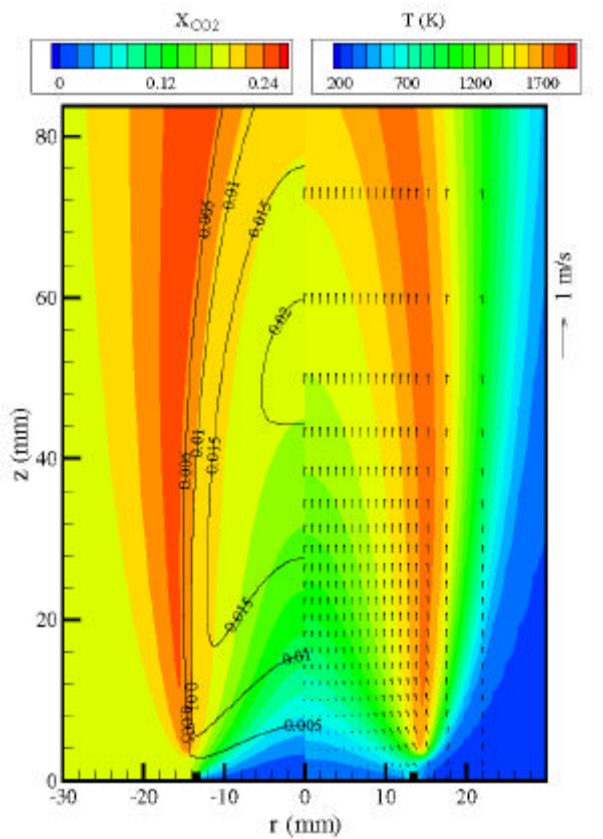


Fig. 13. Cup-burner flame under 0g conditions and with 19.1% CO_2 added to air stream. Calculations were made after ignoring radiative heat losses. Temperature and velocity fields are shown on right half and CO_2 and H_2 concentrations are shown on left half.